

Review

Brookite: Nothing New under the Sun?

Matteo Monai *, Tiziano Montini and Paolo Fornasiero 

Department of Chemical and Pharmaceutical Sciences ICCOM-CNR Trieste URT, Consortium INSTM Trieste Research Unit, University of Trieste, via L. Giorgieri 1, 34127 Trieste, Italy; tmontini@units.it (T.M.); pfornasiero@units.it (P.F.)

* Correspondence: matteo.monai@phd.units.it; Tel.: +39-040-5583973

Received: 2 October 2017; Accepted: 11 October 2017; Published: 13 October 2017

Abstract: Advances in the synthesis of pure brookite and brookite-based TiO₂ materials have opened the way to fundamental and applicative studies of the once least known TiO₂ polymorph. Brookite is now recognized as an active phase, in some cases showing enhanced performance with respect to anatase, rutile or their mixture. The peculiar structure of brookite determines its distinct electronic properties, such as band gap, charge-carrier lifetime and mobility, trapping sites, surface energetics, surface atom arrangements and adsorption sites. Understanding the relationship between these properties and the photocatalytic performances of brookite compared to other TiO₂ polymorphs is still a formidable challenge, because of the interplay of many factors contributing to the observed efficiency of a given photocatalyst. Here, the most recent advances in brookite TiO₂ material synthesis and applications are summarized, focusing on structure/activity relation studies of phase and morphology-controlled materials. Many questions remain unanswered regarding brookite, but one answer is clear: Is it still worth studying such a hard-to-synthesize, elusive TiO₂ polymorph? Yes.

Keywords: TiO₂; brookite; polymorph; polymorphism; photocatalysis

1. Introduction

Polymorphism—the ability of a solid material to exist in more than one crystal structure—is a common property of metal oxides [1]. Different polymorphs have distinct chemico-physical properties, such as electronic and optical properties, magnetism [2], ion conductivity [3], photo/electro-chromism [4], and surface energy and atom arrangement, which in turn affect the material performance in various applications, such as sensing [5] and photocatalysis [6,7]. Rationalizing the effect of crystal structure on the performance of a photocatalytic material is a pivotal research goal, since both Fe₂O₃ and TiO₂, the most investigated and widely used photocatalysts, may exist in different crystal structures [7,8]. Nonetheless, studying such a relation is not a trivial task, because of the many interconnected factors which influence the rate of photochemical reactions (e.g., particle size, shape, crystallinity, number/type of defects, electron-hole recombination, surface area, reactant and intermediate species adsorption on the catalyst surface) and the difficulty of synthesizing materials with a single crystal structure. The latest advances in nanotechnology are shedding new light on the field of photocatalysis, helping to understand the role of crystal structure and morphology in photocatalytic processes.

There are four commonly known polymorphs of TiO₂: anatase (tetragonal), rutile (tetragonal, the most thermodynamically stable phase), brookite (orthorhombic) and TiO₂ (B) (monoclinic) [9]. The structural parameters of these polymorphs are listed in Table 1. Such different lattice structures cause different mass densities and electronic band structures in TiO₂ polymorphs. The exact position of the conduction and valence band edges of TiO₂ polymorphs is still debated, mostly because it is dependent on the purity of the material, its crystallinity and its particle dimensions. While a consensus has been reached for an approximate band gap value, E_g , of anatase (3.2 eV) and rutile (3.02 eV), the

reported experimental E_g values of brookite range from 3.1 to 3.4 eV: both smaller and larger than that of anatase [10]. Even more uncertain is the value of E_g of monoclinic TiO₂ (B), reported in the range of 3.1–4.1 [11–13]. Theoretical approaches (e.g., hybrid functionals, GW methods, the Bethe-Salpeter equation (BSE) method) are also not able to accurately estimate both the fundamental and optical band gap of these materials [10,13,14]. Nonetheless, determining the band gap, the flatband potential and the energy level of trap states, defects and impurities is crucial for the design of materials with improved photocatalytic properties, so future theoretical and experimental detailed studies are needed in order to solve these issues [15].

Table 1. Structural parameters of the main TiO₂ polymorphs. Data reproduce from reference [9], with permission of the American Chemical Society, 2017.

Polymorph	Crystal System	Space Group	Unit Cell Parameters			
			<i>a</i> /nm	<i>b</i> /nm	<i>c</i> /nm	β /degree
anatase	tetragonal	<i>I</i> 4 ₁ / <i>amd</i>	0.379	-	0.951	-
rutile	tetragonal	<i>P</i> 4 ₂ / <i>mnm</i>	0.459	-	0.296	-
brookite	orthorhombic	<i>Pbca</i>	0.918	0.545	0.515	-
TiO ₂ (B)	monoclinic	<i>C</i> 2/ <i>m</i>	1.216	0.374	0.651	107.3

Once considered inactive, brookite is now gaining more and more attention in the field of photocatalysis due to its peculiar performance. A very comprehensive review of brookite was published some years ago by Di Paola et al. [10]. While some detailed reviews on TiO₂ for photocatalytic applications can be found in the literature, focusing on electronic properties [16], exposure of tailored facets [17] and nanostructural control [18]. The present review is focused on the advancement in brookite synthesis for photocatalytic applications, a research field in rapid expansion. First, the most advanced synthetic methodologies to produce pure brookite and well-defined brookite-containing composites are presented, together with some guidelines for thorough characterization of the materials. Then, some applications of brookite as a photocatalyst are outlined in comparison with the performance of other TiO₂ polymorphs. Finally, structure/activity relations are summarized and a perspective on the future development of brookite nanostructured materials is given.

2. Characterization

TiO₂ polymorphs are usually identified by X-ray diffraction (XRD) or Raman spectroscopy. The presence of brookite in a TiO₂ sample can be evidenced by the presence of the characteristic (121) peak at $2\theta = 30.8^\circ$ in the XRD pattern (Figure 1a). While rutile is also straightforward to identify from XRD patterns, thanks to the (110) peak at 27.43° , the detection of anatase in an apparently pure brookite sample is complicated by the overlapping of the (101) main diffraction peak of anatase at 25.28° with the (120) and (111) peaks of brookite, at 25.34° and 25.28° , respectively (Figure 1a). In order to quantitatively assess the phase composition of a TiO₂ sample, the whole XRD pattern should be fitted by a structure refinement method, such as the Rietveld method [19]. The method is very accurate as it allows us to take into account the broadening of the XRD peaks at higher Bragg diffraction angles and the possible preferred crystal orientations in plate- or rod-like crystallites, for which the reflex intensities vary from that predicted for a completely random distribution. In a study by some of the present authors on the synthesis of TiO₂ nanocrystals with precise and tunable exposed facets, the Rietveld method was used in conjunction with simulations and electron microscopy results to determine the phase and the average nanocrystal dimensions [20].

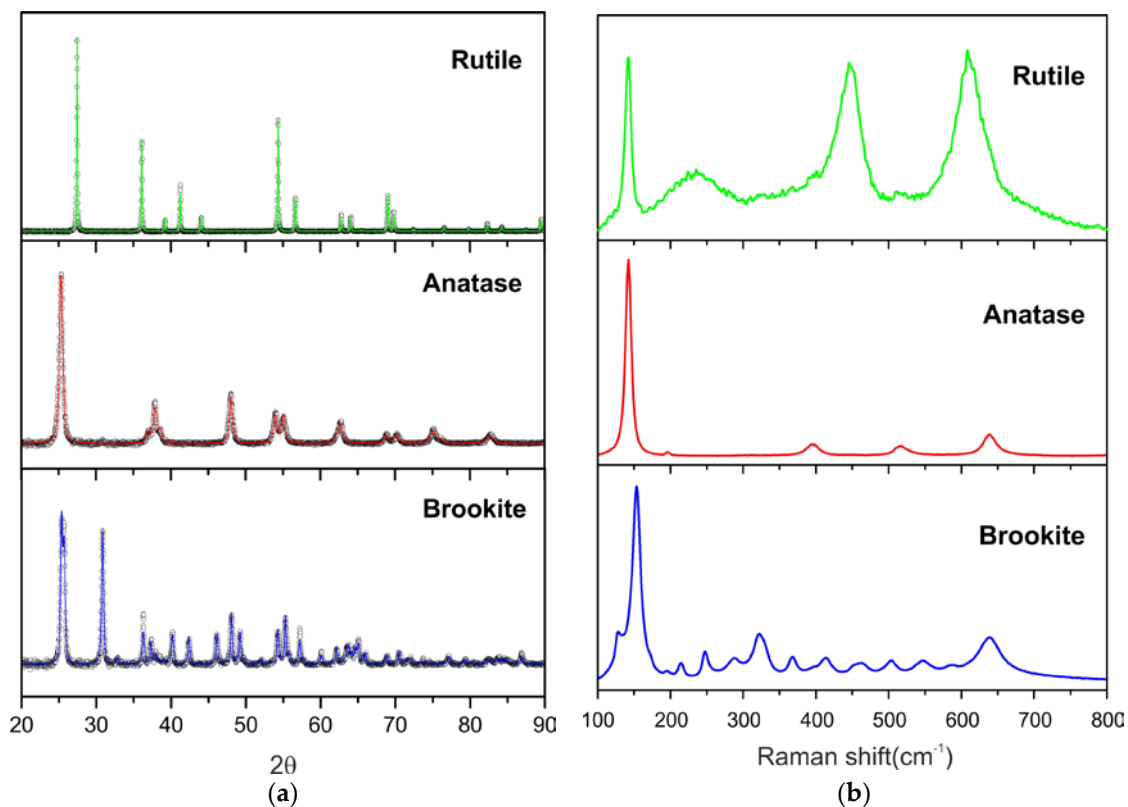


Figure 1. (a) XRD patterns (colored dots) and Rietveld analysis (black lines) of pure rutile, anatase and brookite (reproduced from [21] with the permission of the Elsevier, 2017) and (b) corresponding Raman spectra.

Raman spectroscopy can be used in combination with XRD in order to gain more insight into the phase composition of TiO₂ samples. Raman is very sensitive to minor phase impurities which might go undetected by XRD, and allows spatial mapping in the 10 × 10 micrometer resolution in confocal microscope setups. Since the vibrational spectrum of brookite presents more bands than the other two polymorphs, small amounts of brookite can be detected (Figure 1b) [22]. The more symmetric anatase and rutile structure gives rise to much simpler Raman spectra, with characteristic features evidenced in Figure 1b [23]. Insights into the surface/bulk distribution of phases in a TiO₂ sample can be gained by a combination of common visible/IR Raman with UV Raman spectroscopy, which is more surface-sensitive due to the adsorption of UV light by TiO₂ [24,25]. This approach was used to demonstrate that, in the anatase → rutile transition, rutile forms in the bulk, while anatase can persist on the surface of the sample to higher temperatures than previously thought. Applying this method to the study of brookite-based samples could lead to a deeper understanding of brookite formation and phase transitions.

Transmission electron microscopy (TEM) can provide insights in the phase composition of small areas of the material (hundreds of nanometers in size) by electron diffraction over a selected area electron diffraction pattern (SAED) [26]. In this regard, it can be used in combination with XRD, which gives bulk-sensitive results. Moreover, high-resolution TEM (HRTEM) can reveal the presence of amorphous material, which can be also quantified quite precisely by electron energy loss spectroscopy (EELS), provided that a crystalline and amorphous standard are available [27]. HRTEM can be used to study preferential exposure of facets, crystal morphology, grain boundaries and presence of defects, which can all influence the photocatalytic activity of a material and are therefore very important in structure/activity relation studies. Nonetheless, in some cases it is hard to distinguish between TiO₂ phases, making a definitive assignment difficult if nanocrystals are not suitably aligned with respect to

the electron beam [28]. Moreover, the presence of defects and lattice deformation can lead to slight changes of diffractograms, so intensive characterization is needed in this kind of HRTEM study [26].

Quite interestingly, X-ray absorption spectroscopy (XAS) techniques have seldom been used to study TiO₂ polymorphism [29–31], despite the crystal structure sensitivity of such methods. A reason for this is that XAS techniques are not for routine characterization, since they require access to synchrotron facilities. However, Ti L₃-edge and O K-edge XAS can be used to study the local Ti and O symmetry and to investigate the crystal structure in great detail. For instance, the pre-edge region of the Ti L₃-edge allows accurate quantification of the degree of crystalline nature of a sample, in a more sensitive way than is performed by XRD [30]. Finally, in-situ studies would give new insights into phase transition processes and in structure–activity relations.

Other characterization techniques, not sensitive to phase composition, are nonetheless essential in order to fully characterize and study TiO₂ materials, especially for their use in photocatalysis and to study structure/activity relations. A comprehensive discussion of all such techniques is out of the scope of this paper, but recent reviews on the topic can be found in the literature [32,33].

3. Synthesis

The first synthesis of pure brookite dates back to the 1950s [34]. Since then, a lot of progress has been made in controlling the phase composition of TiO₂ materials, and now a number of synthetic methods exist to produce pure and mixed-phase brookite, rutile and anatase. The effect of the preparation parameters of TiO₂ materials on the final phase composition has also been widely investigated and was recently reviewed by Kumar and Rao [35]. However, the development of new phase-specific synthetic routes remains a trial-and-error process, due to the many thermodynamic and kinetic factors influencing the final phase composition. Indeed, the thermodynamic stability of polymorphs in nanocrystal systems is strongly affected by surface energy contributions, which in turn depend on the nanoparticles size, shape, exposed facets and surface adsorbates, as recently reviewed [36]. Kinetic processes such as reactant diffusion and ripening can be even more influential in particle formation and growth regimes, which usually occur far from equilibrium. The fact that brookite synthesis is more challenging than that of anatase and rutile is due to the narrower energy stability window of brookite compared to other polymorphs.

Moreover, brookite, anatase and monoclinic TiO₂ (B) are all metastable phases, and are transformed to the most thermodynamically stable polymorph—rutile—by annealing at high temperatures. Therefore, post-synthetic temperature treatments, usually employed to improve the degree of crystallization, to reduce the sample or to remove organic precursors, should be carefully controlled in order to avoid the phase transformation of metastable polymorphs. The process of phase transformation has been widely investigated, especially on anatase, but its mechanism is not yet consolidated, to the point that all these transitions were observed: anatase to brookite to rutile [37], brookite to anatase to rutile [38], anatase to rutile [39,40], and brookite to rutile [41]. This is due to the fact that the phase transformation process depends on many factors, such as starting material, temperature, particle size, surface area [37], surface defect sites and presence of adsorbates [42]. The transformation sequence was rationalized in terms of surface enthalpy crossover upon coarsening [37], but further studies are needed in order to shed some light on such a complex process.

Hydrothermal methods are the most commonly employed to synthesize brookite. Briefly, a TiO₂ precursor is mixed with water or organic solvents, an acid or base and additives such as capping/chelating agents or salts, and heated in an autoclave to moderately high temperatures and pressures. Typical Ti precursors are chlorides (TiCl₃, TiCl₄), Ti(SO₄)₂, alkoxides (e.g., isopropoxide, butoxide), alkaline titanates and amorphous titania. In general, there is no one-fit-all strategy in order to obtain brookite; acidic or basic conditions can be employed to obtain pure brookite, depending on the set of conditions, and additives which are necessary in one case can be avoided by changing other synthetic parameters. Nonetheless, varying the reaction parameters in a systematic way, different polymorphs can be obtained [43,44].

Adapting the procedure reported by Zhao et al. [45], some of us showed that pure brookite, anatase and rutile with a well-defined shape and dimension can be obtained using titanium (IV) bis(ammonium lactate) dihydroxide, $\text{Ti}(\text{NH}_4\text{C}_3\text{H}_4\text{O}_3)_2(\text{OH})_2$, and varying the concentration of urea in aqueous solution (0 to 7.0 M) at 160 °C for 24 h (Figure 2). Pure brookite nanorod formation was favored by higher urea concentrations, corresponding to higher pH values due to urea decomposition, in accordance with the literature [45,46]. Interestingly, the use of comparable urea concentrations to those reported by Zhao et al. resulted in slightly different phase compositions of the final material, probably because of the influence of setup parameters such as autoclave free volume and heating/cooling method [21].

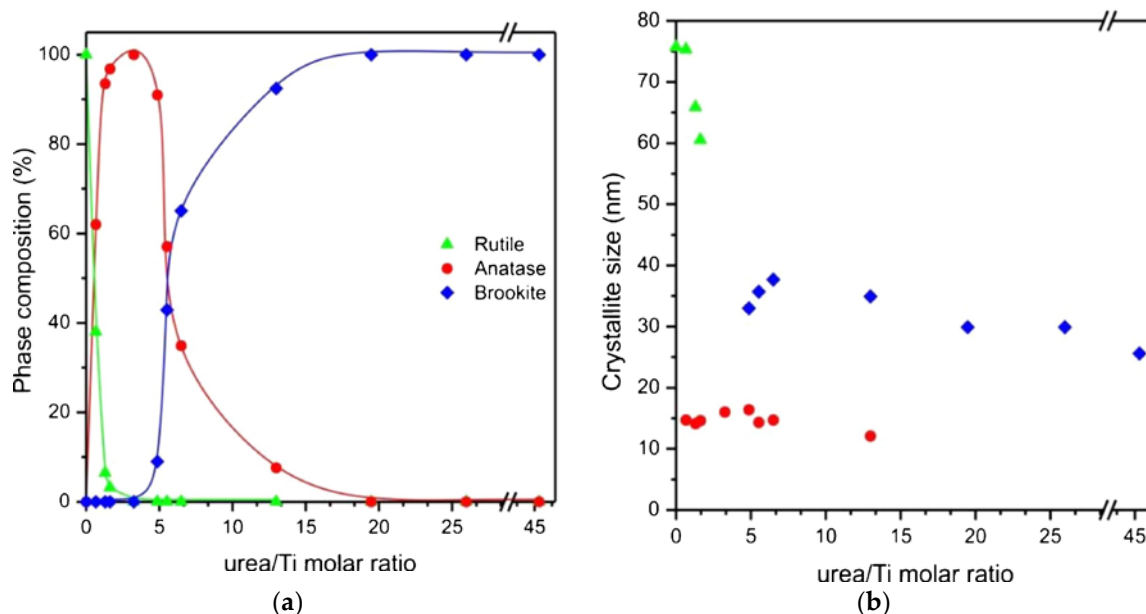


Figure 2. (a) Evolution of phase composition and (b) mean crystallite sizes as a function of the initial urea concentration. Reproduced from reference [21] with the permission of the Elsevier, 2017.

The drawbacks of hydrothermal synthesis are high energy consumption, low throughput and of difficult scalability due to the high pressure and temperature conditions of the sealed synthesis vessel, which also makes in-situ monitoring of the synthesis a challenging task. However, to the best of our knowledge, pure brookite has not been synthesized so far by other wet-chemistry methods, such as sol-gel, ionic liquids assisted synthesis, ultrasound and microwave-assisted synthesis and microemulsion [35,47]. The reason for this is most probably related to the aforementioned narrower stability window of brookite compared to other polymorphs, but this aspect surely deserves more investigation in the future.

Mechanochemical activation methods, such as ball milling (BM), are emerging as more sustainable synthetic methods because of the absence of bulk solvents and the possibility to use metal oxides or hydroxides as starting materials [35,48]. While pure brookite synthesis by BM has not been reported so far, future studies could clarify the role of the reaction parameters on the phase composition of the final material. Moreover, brookite could be used as a starting material in BM synthesis in order to study its stability (and therefore the feasibility of the synthetic method) and the phases formed under different conditions.

Modification of TiO_2 by doping (H, N, C, metal ions), co-doping and self-doping (Ti^{3+} , black titania [49]) are general strategies to enhance TiO_2 light harvesting and photocatalytic properties. Doped brookite synthesis by the introduction of dopants or their precursors in brookite hydrothermal synthesis was recently reported [10]. As suggested by a computational study of TiO_2 polymorphs (H,N)-co-doping, the effect of doping on the electric properties of anatase, rutile and brookite can be

different. For instance, (H,N)-co-doping reduced the band gap of anatase and brookite, but had little effect on rutile [50]. Combined experimental and theoretical results on this topic could greatly extend our knowledge of TiO₂, and some efforts have been recently spent in this sense [51].

Self-doping of TiO₂ by Ti³⁺ can be accomplished by various reduction methods, using plasma or thermal, chemical or electrochemical activation [49]. With the intent of avoiding harsh, harmful and expensive methods, recent studies focused on the development of yet other synthetic routes [52,53]. For instance, pure black brookite synthesis was recently reported, in which melted Al was used as a reducing agent in a two-zone vacuum furnace, instead of employing more dangerous H₂ [52]. In this case, the Al reduction reportedly starts from the brookite surface and causes lattice disorders and oxygen vacancies in the surface layer. Xi et al. reported a hydrothermal synthesis of black brookite using post-annealing treatment in order to introduce large amount of Ti³⁺ defects in the bulk of the nanoparticles [53]. Interestingly, no rutile or anatase were detected after N₂ annealing treatment at elevated temperatures (up to 700 °C), suggesting that brookite can be stabilized by reduction. Systematic studies comparing different synthetic routes are greatly desired, since the synthetic method can affect the properties and performances of black TiO₂ materials, leading to the diverse results rationalization found in the literature [49]. Controlling the amount and spatial distribution of surface lattice disorder, oxygen vacancies, Ti³⁺ ions, Ti–OH and Ti–H groups present in black TiO₂ would also open the way to band-gap engineering in order to enhance photocatalytic performances in targeted reactions.

Finally, in order to scrupulously study structure/activity relations in TiO₂ materials, the synthesized samples should not only have controlled phase composition, but also well-defined crystallite dimensions and morphology. Indeed, different facets of TiO₂ crystals have distinct photocatalytic properties as a result of different atomic and electronic structure [17,54]. The nanostructure also plays a pivotal role in photocatalysis. For instance, the rate of electron–hole recombination in brookite nanorods can be controlled by engineering their length, as recently reported by some of us [28]. The synthesis of nanostructured TiO₂ has been widely investigated in the literature [18,20,55], so that a wide library of morphology-controlled materials can now be produced. Structure/activity studies on TiO₂ are thriving, as they can provide great insights into reaction mechanisms and give an indication of how to enhance the performance of state-of-the-art photocatalysts.

4. Photocatalytic Studies

The phase composition of TiO₂ nanomaterials is one of the factors strongly influencing photocatalytic reaction activity and selectivity [56]. This is mainly due to the phase-dependency of electronic structures (band gap, charge-carrier lifetime and mobility, exciton diffusion length, trapping sites) and of preferentially exposed surfaces with different energy, atom arrangements and adsorption sites. While anatase- and rutile-based nanomaterials have been widely investigated and their photocatalytic performances are well established [9,17], brookite has slowly gained the status of an efficient photocatalyst only in the last couple of decades, as recently reviewed [10]. Here, we report the latest advances in photocatalysis over brookite-based materials, focusing on comparative and in-depth studies, to give a critical view of the present challenges in structure/activity relation studies.

One of the reasons for the different photocatalytic performances of TiO₂ polymorphs is the trapping of photogenerated charge carriers (electrons and holes) in defect sites, resulting in slower electron-hole recombination kinetics and phase-dependent charge carrier stabilization. The density of such occupied mid-gap trap states (DOTS) can be studied by time-resolved vis-IR absorption spectroscopy (TRAS) [57,58]. In a recent experimental study, the depth of electron-traps in brookite was estimated to be 0.4 eV, which is deeper than that of anatase (<0.1 eV), but shallower than that of rutile (~0.9 eV) [57]. These results are in good accordance with the calculated stabilization energies for rutile (0.8–1 eV) and anatase (0–0.2 eV), in which oxygen vacancies or interstitial Ti atoms were considered as trap site defects [59,60]. Notably, to the best of our knowledge, no theoretical study has

been reported on electron trapping at the defects of brookite, even if similar results to anatase and rutile are expected. Some of the authors recently reported a study on trapped carriers in different TiO₂ polymorphs in the ms–s timescales, typical of photocatalytic reactions [58]. Also in these slow timescales, anatase and brookite exhibit dispersive power law recombination dynamics, in accordance with shallow charge trapping, while rutile exhibits logarithmic decay kinetics, indicative of deeper charge trapping.

The stabilization of electrons in trap states has two opposite effects: on the one side, it reduces the reactivity of electrons, and on the other, it causes an increase in the lifetime of electrons and holes, because the probability of recombination is decreased. Therefore, an appropriate electron trap depth can help in maximizing the yield of long-lived, but still reactive, charge carriers. In the presence of traps of moderate depth, such as in brookite, electrons can take part in reduction reactions, while long-lived holes can participate in photocatalytic oxidation reactions, such as water oxidation (Figure 3). In anatase, the trap-depth is too shallow to extend the lifetime of holes, while in rutile it is too deep for electron-consuming reactions (Figure 3). Notably, deep electron trapping in rutile extends the lifetime of holes, which could promote water oxidation. However, the low reactivity of deeply trapped electrons causes the overall activity to be low [61].

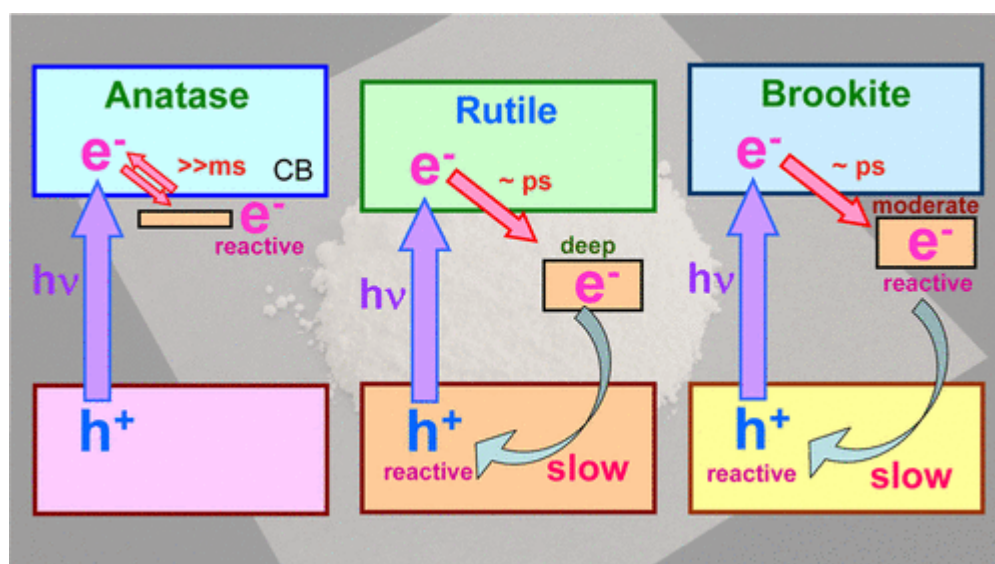


Figure 3. Schematic representation of electron trapping sites in anatase, rutile and brookite. CB: conduction band. Reproduced from reference [57] with permission of the American Chemical Society, 2017.

Particle size can also have a great influence on photocatalytic activity due to geometric and electronic effects. While a smaller particle size results in larger surface areas (which means more active sites per volume) and shorter mean distances for carriers to migrate to the surface, it also brings about some drawbacks such as less volume to generate and separate charge carriers, an increase of band gap due to quantum confinement and incomplete band relaxation to the bulk level (which means a smaller potential drop and electric field in the space charge region, and hindered charge separation) [62]. Therefore, a compromise in particle size between the positive influence of having more reactive sites and the negative influence of increased recombination is wanted. Nonetheless, electron-hole separation can be improved by controlling the morphology of nanocrystals, while maintaining high specific surface areas.

As recently demonstrated by some of the authors by a combination of electron paramagnetic resonance (EPR) spectroscopy and in-situ TRAS [28], H₂ production rates in the photoreforming of ethanol, glucose and glycerol increases with the increasing length of Pt-decorated brookite nanorods

due to the longer lifetime of charge-separated states (Figure 4). A broad photoinduced absorption feature in the visible range is obtained in TRAS when pumping above the brookite band gap, which was assigned to trapped holes lying energetically within the band gap and physically on or near the surface of the TiO₂ nanoparticles [63]. The TRAS normalized kinetics reported in Figure 4 show an ultrafast rise due to the trapping of photoexcited holes of the order of a few hundred fs, followed by a decay due to the recombination of holes with electrons or reaction with adsorbates. The increase in the lifetime of the trapped holes with nanorod length was attributed to the different surface energy of crystal faces exposed on the tips and the sides of the nanorods, which drives the electrons and holes to different crystal faces, leading to enhanced charge carrier separation in longer nanorods [64]. Studies of photocatalytic coupling of methanol to methyl formate and the photo-oxidation of acetaldehyde to acetate on brookite nanorods revealed similar length-dependent rate enhancement, corroborating the proposed model [65].

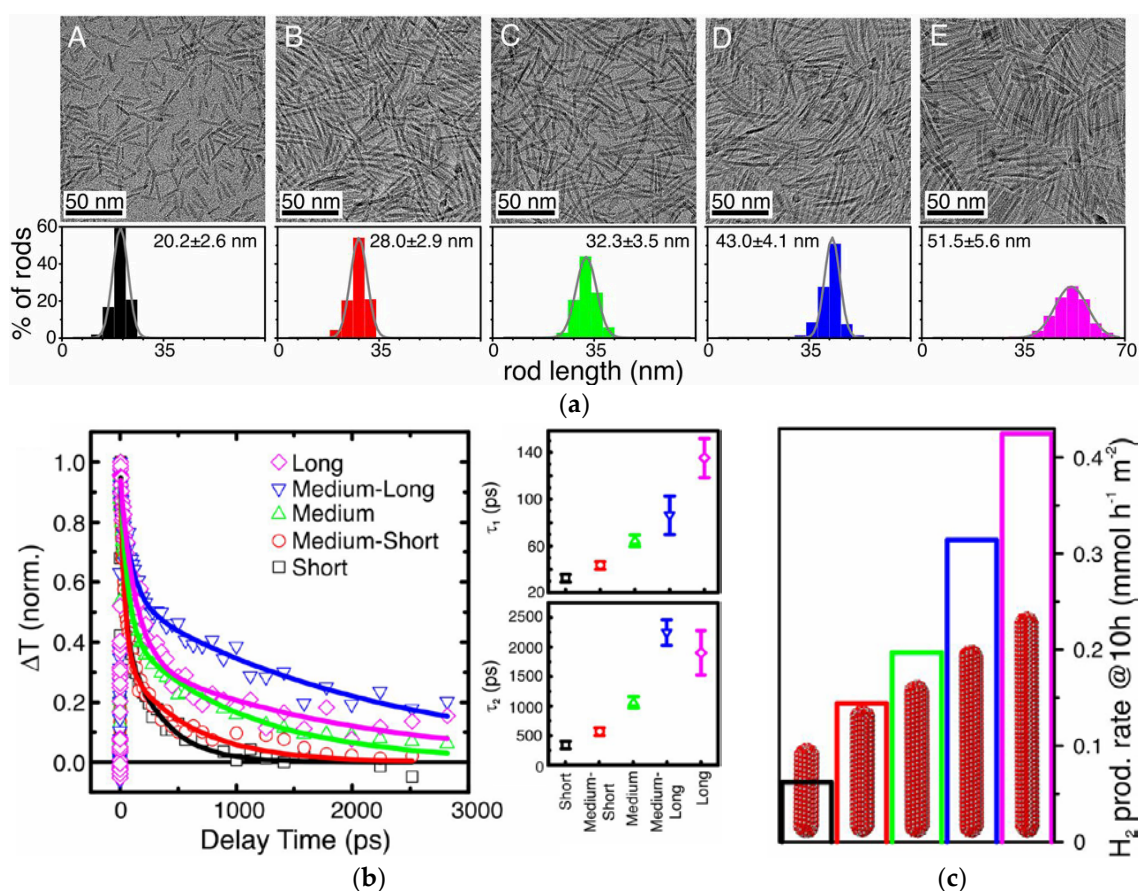


Figure 4. (a) TEM images and size analysis for the brookite nanorods with different lengths; (b) Normalized TRAS (time-resolved vis-IR absorption spectroscopy) kinetic traces of Pt-decorated nanorods in ethanol. Insets show fitted time constants (τ_1 (Top) and τ_2 (Bottom)); (c) H₂ production rates from ethanol photoreforming on 1 wt. % Pt–brookite nanorods of different length after 10 h under illumination, normalized by the surface area of the photocatalysts. Reproduced from reference [28] with the permission of the PNAS, 2017.

The EPR results further indicated that electrons in longer nanorods transfer to Pt faster than electrons in shorter nanorods. The capture of electrons by Pt increases the lifetime of the charge-separated state, as indicated by the much faster decays observed for nanorods without Pt in ethanol [28]. A similar effect was observed for Au surface decoration of brookite nanorods [66], which enabled electrons a lifetime of four orders of magnitude longer due to efficient hopping on brookite

lateral facets. Conversely, when Au nanoparticles are introduced in the bulk of nanorods, they act as recombination centers for plasmonic carriers in the fs timescale.

From the above discussion, it is clear that the control over exposed crystal faces is an essential aspect in fundamental photocatalytic studies, as the surface energy, chemical surface state, number/type of defects and reactivity strongly depend on the atomic arrangement of the exposed surfaces [17,54,67,68]. In the last decade, the synthesis of TiO₂ anatase, rutile and brookite nanocrystals with controlled exposed faces has been reported by several groups, employing specific precursors/conditions or suitable structure-directing agents. All polymorphs show pronounced structure/activity relations, with distinct crystal faces showing dramatically different reactivity and specifically promoting reduction or oxidation [64]. Ohno et al. reported clear evidence of such face-dependent reactivity by studying the photodeposition of Pt (by reduction of PtCl₆[−]) and of PbO₂ (by oxidation of Pb²⁺ nitrate) on rutile, anatase [69], and brookite [68,70]. On brookite TiO₂ nanorods, reduction and oxidation reactions were observed to proceed predominantly on {210} and {212} exposed crystal faces, respectively [68,70]. In brookite nanosheets, {201} facets acted as oxidation sites, while {210} and {101} facets acted as reduction sites [64]. Face-specific reactivity was also employed to selectively modify the tips of brookite nanorods with Fe³⁺ ions, to enhance the activity in acetaldehyde photocatalytic oxidation [68].

Theoretical studies also evidenced the importance of the energetics of crystal faces. The sequence of surface energies of ten stoichiometric 1 × 1 low-index surfaces of brookite was calculated by first-principle density functional theory (DFT) simulations, showing that the electronic and chemical properties of brookite and the other TiO₂ phases can be significantly different [67]. Recently, combined theoretical and experimental studies of brookite nanomaterials demonstrated that preferential exposure of {121} faces, with under-coordinated atoms and lower VB potential, led to higher performance in photodegradation, while preferential exposure of {211} surface, with higher CB potential, resulted in enhanced H₂ productivity [71,72]. Such calculations also suggested that electrons struggle to migrate from bulk to {121} faces, in accordance for their poor H₂ production efficiency.

While pure phase TiO₂ materials are extensively investigated for fundamental studies, mixed phase TiO₂ materials have been shown to provide enhanced photocatalytic performances, due to charge transfer across the interface of different phases [73]. For instance, the widely investigated TiO₂ Degussa P25, used as a standard in the majority of TiO₂-related studies, is a mixture of anatase and rutile particles (anatase/rutile ratio ~70:30) in which a synergistic effect of the two phases is ascribed to the spatial separation of photogenerated charge carriers [74]. Despite the general consensus in such mechanisms, there is disagreement about the direction of charge transfer, which depends on the relative positions of the conduction bands and trap states in the two polymorphs. Electron transfer from anatase to rutile was proposed by Kawahara et al., based on results of the photodeposition of Ag on a patterned bilayer-type TiO₂ photocatalyst consisting of anatase and rutile phases [75]. SEM images clearly showed silver particles mostly deposited on the anatase surface, except at the interfacial region, in which silver deposition occurred preferentially at the rutile layer boundary, suggesting electron transfer from anatase to rutile. On the other hand, the opposite mechanism was proposed by other studies basing on EPR spectroscopy results, in which photogenerated electrons migrated from rutile to anatase trapping sites [74,76].

Recently, a similar enhancement of photocatalytic activity in the photodegradation of organic molecules and CO₂ photoreduction has been also observed for brookite/anatase [45,77,78] and brookite/rutile mixtures [79,80]. Moreover, anatase-rich/brookite mixture (75:25) was shown to be much more active for CO₂ photoreduction than Degussa P25, an anatase-rich/rutile mixture with similar anatase fraction [45]. These results suggest that electron transfer may take place also in brookite-based TiO₂ composites, which may be a new direction for the development of efficient photocatalysts. However, to the best of our knowledge, no direct evidence for electron transfer, e.g., by EPR, has been reported so far. DFT calculations on pairs of rutile, anatase and brookite TiO₂ slabs showed that in most cases highest occupied molecular orbital (HOMO) and lowest unoccupied

molecular orbital (LUMO) states were separated in the two phases, indicating that charge transfer may take place upon photoexcitation [81]. Such separation was observed to be dependent on the native HOMO–LUMO states of the two components used to build the composites and on the lattice match between the surfaces of the two phases. Future experimental and theoretical investigations focused on the structural and electronic properties of brookite TiO₂ composite interfaces are needed to gain further insights into efficient photocatalyst preparation. On the other hand, since the presence of interfaces can drastically improve the activity of TiO₂ materials, careful characterization is essential to rule out contamination in fundamentals studies aimed to assess the differences in the activity of polymorphs.

It should be noted that the relative activity of polymorphs is dependent on the considered photocatalytic reaction, so that a general activity trend among brookite, anatase and rutile (and their composites) does not exist [82,83]. For instance, two distinct activity trends were observed for anatase, brookite and their composites in MeOH photoreforming and in dichloroacetic acid (DCA) degradation [82]. This was explained by two different rate-determining factors: H₂ production was favored by the cathodically-shifted flatband potentials of brookite materials with respect to anatase, while DCA degradation rates were highest for anatase, and observed to increase with surface area (Figure 5a). Organic degradation studies can be further complicated by a non-trivial effect of calcination temperature and the sorption capacity of ions and of dissolved gases (e.g., O₂) in water on the relative activity of brookite and anatase [83]. Normalizing the photocatalytic activity by a certain value may help in rationalizing the results, as observed by normalization to initial absorbed Ag(I) or Cr(VI) amount [83] and by normalization to the surface area in anatase/brookite materials used in photocatalytic reforming of ethanol and glycerol [21]. In the latter case, the activity normalized to the surface area continuously increased with the brookite content, indicating that the exposed facets of brookite nanorods possess an intrinsic higher activity in H₂ production than that of the other polymorphs (Figure 5b,c) [21].

Some insights in the factors determining the high intrinsic activity of brookite surfaces come from DFT calculations on the structure and adsorption properties of brookite (210) and anatase (101) surfaces, the most commonly exposed facets in nanocrystals [84,85]. The two surfaces are structurally similar, but the brookite (210) surface presents shorter interatomic distances and a different block arrangement. These features result in enhanced reactivity toward strong dissociative adsorption of H₂O and HCOOH, and generate highly active junction sites, all factors entailing higher specific activity of brookite (210) surfaces [84]. On the other hand, charge analysis calculations revealed that CO₂^{•−} radical anion (the first intermediate in CO₂ reduction) formed on the negatively charged anatase (101) surface, but not on the negatively charged brookite (210) surface, indicating that brookite is not a suitable catalyst for CO₂ reduction [85]. Nonetheless, the study confirmed the previous results on the favorable adsorption energetics of brookite (210), and revealed that the presence of oxygen vacancies on the brookite (210) surface enhanced the charge transfer to the CO₂ molecule, promoting CO₂^{•−} radical formation and CO₂ reduction.

These results were supported by in-situ diffuse reflectance infrared Fourier transform spectroscopy (DRIFTS) and CO₂ photoreduction photocatalytic experiments on defect-free and oxygen-deficient brookite, anatase and rutile TiO₂ nanocrystals [86]. Oxygen vacancies (V_O) and Ti³⁺ sites were created by helium pretreatment of the as-prepared TiO₂ at a moderate temperature on anatase and brookite, but not on rutile. The production of CO and CH₄ from CO₂ photoreduction was remarkably enhanced on defective anatase and brookite TiO₂ (up to 10-fold enhancement) as compared to the defect-free surfaces, thanks to enhanced light harvesting and CO₂ adsorption on defect sites. Defective brookite was the most active photocatalyst among the investigated TiO₂ polymorphs, which was tentatively explained by the favored formation of oxygen vacancies, faster reaction rate of CO₂[−] with adsorbed H₂O or surface OH groups, and an additional reaction route involving an HCOOH intermediate. High CO₂ photoreduction rates were also observed for defective brookite nanosheets with Ti³⁺ self-doping, synthesized by an innovative hydrothermal method combined with post-annealing treatment, avoiding commonly employed harsh and costly physical methods [53]. Defective brookite nanomaterials are

surely worthy of more extensive investigation, in terms of the development of new synthetic routes and of in-depth characterization (e.g., by EPR [87,88]) and photocatalytic studies.

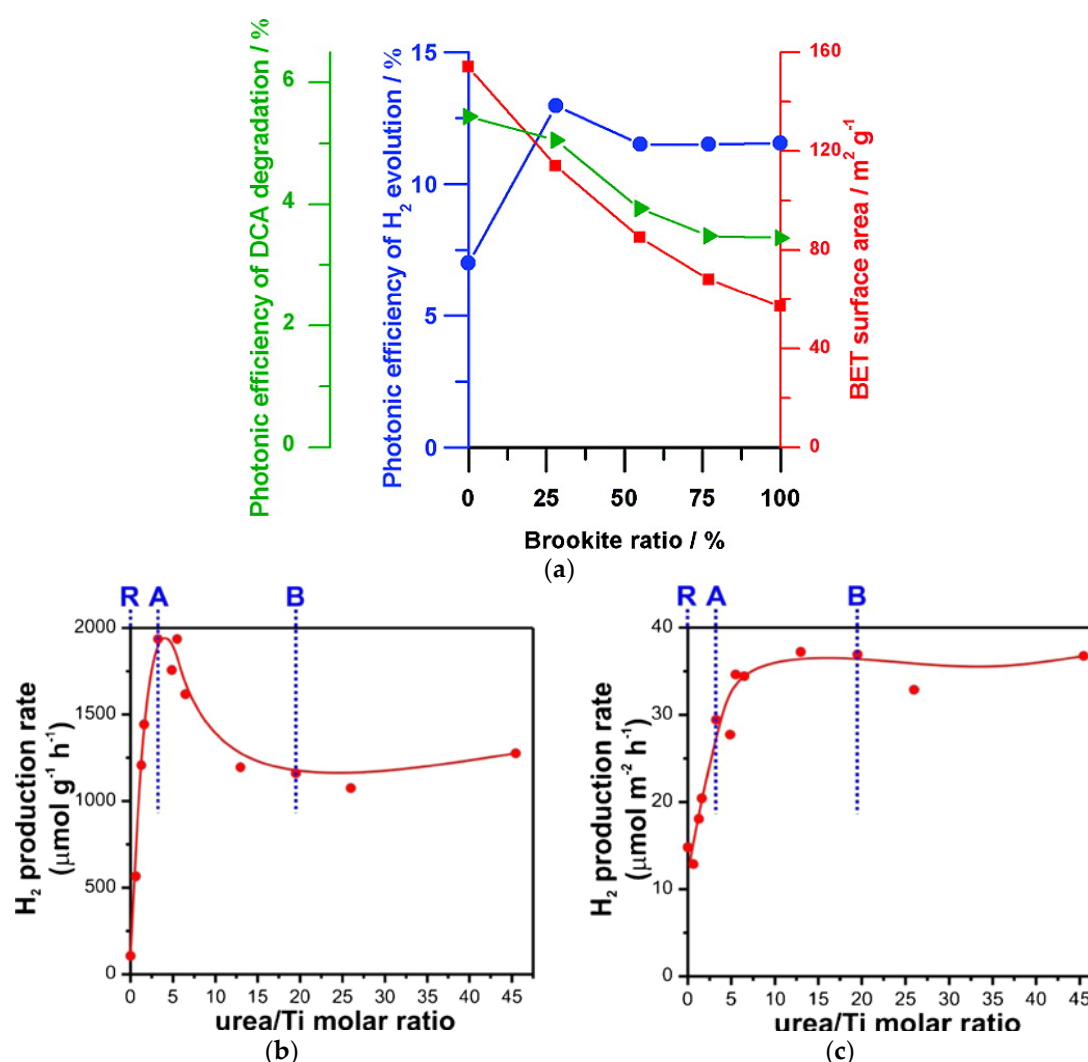


Figure 5. (a) Effect of brookite ratio on the photonic efficiency of TiO₂ composites in dichloroacetic acid (DCA) degradation (green triangles) and H₂ production (blue circles). BET surface area (red squares) is reported for comparison with the efficiency trends. Reprinted with permission of reference [82]; (b) H₂ production rate by photocatalytic ethanol dehydrogenation over Pt(0.2 wt. %)/TiO₂ prepared using different urea/Ti molar ratios, normalized with respect to the mass of catalysts and (c) with respect the surface area. Markers correspond to the urea/Ti molar ratios that allow the preparation of pure phase materials: rutile (R), anatase (A) and brookite (B). Reproduced from reference [21] with permission of the American Chemical Society, 2017.

Selectivity studies in photocatalysis have long been lacking, but are now gaining momentum due to the significant advantages presented by photocatalytic reactions as alternative, green routes in organic and inorganic chemistry [89]. The selectivity of photocatalytic systems can be enhanced by two main strategies: modification of the photocatalyst and optimization of reaction conditions (e.g., aeration, type of solvent, concentration and type of anions [90], use of membranes) [91]. Not surprisingly, the TiO₂ phase composition was demonstrated to have an effect on the selectivity of many photocatalytic reactions, such as ammonia oxidation [92], photoinduced decomposition of acetone, oxygenate photoreforming [6], and selective oxidation of alcohols to aldehydes [91,93]. For instance, the product distribution of ammonia oxidation was different in the case of rutile, yielding

nitrites as a major product, and of anatase and brookite, yielding mild-oxidation products such as nitrites and N_2 [92]. In a study by some of the authors, brookite was observed to be less active in the complete mineralization of glycerol during photocatalytic reforming, leading to higher H_2/CO_2 and opening interesting opportunities in selective oxidation of sacrificial agents. On rutile, on the other hand, a selective dehydrogenation of glycerol through the secondary OH group was observed (although with very low activity) [6]. Furthermore, brookite nanorods were observed to selectively produce H_2O_2 , a high value-added and green oxidant, during photoelectrochemical water splitting, also showing a very low onset potential for water oxidation ($E_{onset} \sim -0.2$ V vs. reversible hydrogen electrode (RHE)) [66]. These findings suggest that the effect of TiO_2 phase composition should be investigated more in detail in the highly novel field of selective photocatalysis.

Future theoretical and experimental studies on well-defined nanostructured TiO_2 materials will be essential to unravel the conundrum regarding the relative photocatalytic performances of different polymorphs and their mixtures, considering the discrepancies observed in the literature. We strongly advise the pursuit of rigorous studies of the electronic structure of TiO_2 nanomaterials and of their facet-specific properties, which requires the development of precise and tunable synthesis methods, yielding size and morphology-controlled materials. The task is arduous, but can be now undertaken using the tools of simulations, high-throughput synthesis and nanotechnology.

5. Conclusions and Perspectives

Brookite-based materials are receiving increasing attention in photocatalytic and related applications, due to their novelty and peculiar properties. This "brookite rush" is rapidly producing new evidence of the profound influence of phase composition on photocatalytic activity and selectivity, unraveling the mechanistic aspects and structure/activity relations in photocatalytic processes. Nonetheless, we are still fumbling around in the dark regarding the paramount electronic properties of brookite (e.g., its energy gap), so further theoretical and experimental studies are needed in order to reach a new level of understanding and a wide consensus in the scientific community on this topic. However, the solid research work previously published on anatase and rutile seems to have discouraged similar fundamental investigation of brookite. A prime example of this is the case of the postulated electron transfer in the brookite/anatase and brookite/rutile interfaces, which was not supported by direct evidence, since similar work was done for anatase/rutile composites [45,77–80]. While such electron transfer is reasonably expected, more caution should be taken in future studies of brookite.

An intrinsic burden to the development of a wide range of morphology-controlled brookite nanomaterials is posed by the limited understanding of solvothermal synthetic mechanisms. This is a common issue in the synthesis of nanomaterials, usually carried out by a trial-and-error approach. Nonetheless, nanostructured brookite (e.g., nanorods [28], nanosheets [64], and nanocubes [94]) has been successfully synthesized, and alternative strategies are being proposed to produce highly-oriented brookite and TiO_2 nanoparticles with the desirable specific external crystal facet (e.g., templating with graphene [95] or 2D oxides [96]). The playground is now open to new areas of investigation, such as the development of scalable and sustainable brookite synthesis, modification by doping [10,50–53], controlled introduction of defects, and synthesis of brookite nanocomposites [94,97] and hybrid organic-inorganic systems [98]. In particular, the effect of TiO_2 phase composition in nanocomposites with metal organic frameworks (MOFs), quantum dots and nanocarbons is still to be assessed. The formation of phase-dependent charged interfaces in such hierarchically-structured materials could be a promising strategy for the design of improved photocatalysts [62].

Investigation of new composites could lead to a great enhancement of photocatalytic performance, stimulating further advances in synthetic methods, characterization techniques and elucidation of catalytic mechanisms. For instance, a non-trivial influence of co-catalyst loading on CO_2 photoreduction activity and selectivity was recently reported for brookite nanocubes loaded with Ag nanoparticles [94]. A maximum yield of CO was observed for 0.5 wt. % Ag loading, which

corresponded to the case of the preferential deposition of Ag nanoparticles on {210} faces, while for intermediate loadings (1 wt. %) of Ag, the CH₄ selectivity increased, due to an agglomeration of Ag on {210} faces and the deposition of small nanoparticles on {001} faces (Figure 6). These fascinating results were tentatively rationalized in terms of an interplay of charge transfers, adsorption properties and light harvesting effects, revealing how the synergistic effects in semiconductors/co-catalyst systems are much more complex than expected, and how they can be used to finely tune the performances of photocatalytic systems.

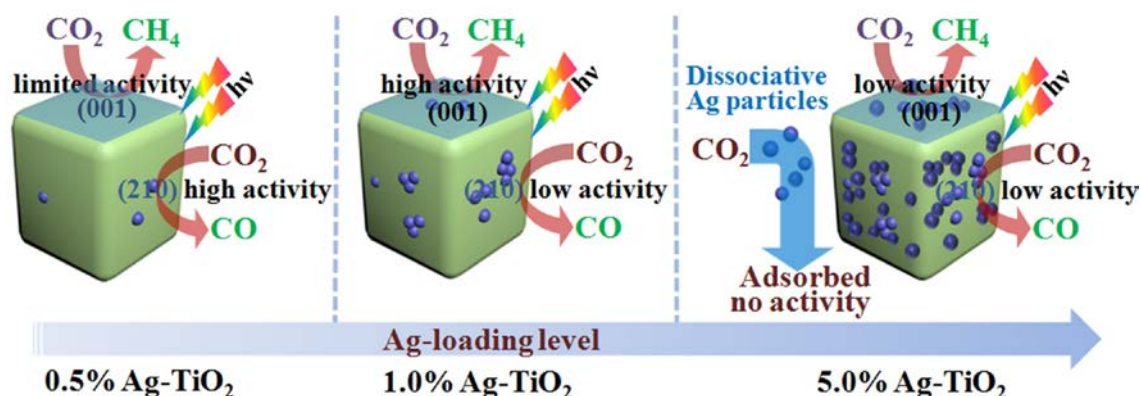


Figure 6. Graphical representation of the influence of Ag co-catalyst wt. % content on the CO₂ photoreduction activity of brookite nanocubes. Reproduced from reference [94] with permission of the Elsevier, 2017.

In-depth studies concerning different band gap and trap states, face reactivity, the effects of crystal morphology and dimension, the presence of vacancies, and the generation of adsorbates and radicals are of great interest, and recently great progress has been made in the study of these properties. Photo-induced heterogeneous electron transfer (ET) across the semiconductor and adsorbed molecules, leading to the formation of radicals (e.g., •OH) is of particular relevance for any photocatalytic reaction, but studying such highly reactive species is challenging [91,99]. An emerging approach is based on the use of organic dye probes in microscopic fluorescence imaging, for the sensitive detection of reactive oxygen species, their diffusion in solution or air, and the identification of photocatalytic active facets on semiconductor surfaces [100,101]. Recently, a mass spectrometry-based approach was used to investigate the ultrafast ET of photoelectrons generated by ultraviolet irradiation on the surfaces of semiconductor nanoparticles or crystalline facets, providing a new technique for studying the photo-electric properties of various materials [102]. Similar studies of brookite would lead to a deeper understanding of the reaction mechanism and provide valuable insights into strategies to enhance activity and selectivity in many photocatalytic reactions.

The phase-dependent activity and selectivity observed in photocatalytic reactions over brookite, rutile and anatase is probably the most exciting and yet still not well investigated aspect concerning TiO₂ polymorphs. Brookite nanomaterials were found to perform better than other polymorphs in various photocatalytic reactions (e.g., CO₂ photoreduction [86,103], photoreforming of oxygenates [21,82], ammonia oxidation [92]), and showed promising properties for future applications also in other fields, such as photoelectrochemical devices [66], dye-sensitized solar cells (DSSC) [104,105], bio-applications and self-cleaning materials [106,107]. The days in which brookite was considered just an undesirable byproduct are long gone, it is now time to dig deeper and find out even more about this and other less familiar TiO₂ polymorphs.

Acknowledgments: Matteo Monai, Tiziano Montini and Paolo Fornasiero acknowledge financial support from the University of Trieste through the FRA2015 project and ICCOM CNR.

Author Contributions: Matteo Monai, Tiziano Montini and Paolo Fornasiero wrote the paper.

Conflicts of Interest: The authors declare no conflict of interest. The founding sponsors had no role in the design of the study; in the collection, analyses, or interpretation of data; in the writing of the manuscript, and in the decision to publish the results.

References

1. Sood, S.; Gouma, P. Polymorphism in nanocrystalline binary metal oxides. *Nanomater. Energy* **2013**, *2*, 82–96. [[CrossRef](#)]
2. Machala, L.; Tuček, J.; Zbořil, R. Polymorphous Transformations of Nanometric Iron(III) Oxide: A Review. *Chem. Mater.* **2011**, *23*, 3255–3272. [[CrossRef](#)]
3. Laarif, A.; Theobald, F. The lone pair concept and the conductivity of bismuth oxides Bi₂O₃. *Solid State Ion.* **1986**, *21*, 183–193. [[CrossRef](#)]
4. Quintana, A.; Varea, A.; Guerrero, M.; Suriñach, S.; Baró, M.D.; Sort, J.; Pellicer, E. Structurally and mechanically tunable molybdenum oxide films and patterned submicrometer structures by electrodeposition. *Electrochim. Acta* **2015**, *173*, 705–714. [[CrossRef](#)]
5. Prasad, A.K.; Kubinski, D.J.; Gouma, P.I. Comparison of sol–gel and ion beam deposited MoO₃ thin film gas sensors for selective ammonia detection. *Sens. Actuators B Chem.* **2003**, *93*, 25–30. [[CrossRef](#)]
6. Beltram, A.; Romero-Ocaña, I.; José Delgado Jaen, J.; Montini, T.; Fornasiero, P. Photocatalytic valorization of ethanol and glycerol over TiO₂ polymorphs for sustainable hydrogen production. *Appl. Catal. A Gen.* **2016**, *518*, 167–175. [[CrossRef](#)]
7. Carraro, G.; Maccato, C.; Gasparotto, A.; Montini, T.; Turner, S.; Lebedev, O.I.; Gombac, V.; Adami, G.; Van Tendeloo, G.; Barreca, D.; et al. Enhanced Hydrogen Production by Photoreforming of Renewable Oxygenates Through Nanostructured Fe₂O₃ Polymorphs. *Adv. Funct. Mater.* **2014**, *24*, 372–378. [[CrossRef](#)]
8. Schneider, J.; Matsuoka, M.; Takeuchi, M.; Zhang, J.; Horiuchi, Y.; Anpo, M.; Bahnemann, D.W. Understanding TiO₂ Photocatalysis: Mechanisms and Materials. *Chem. Rev.* **2014**, *114*, 9919–9986. [[CrossRef](#)] [[PubMed](#)]
9. Ma, Y.; Wang, X.; Jia, Y.; Chen, X.; Han, H.; Li, C. Titanium Dioxide-Based Nanomaterials for Photocatalytic Fuel Generations. *Chem. Rev.* **2014**, *114*, 9987–10043. [[CrossRef](#)] [[PubMed](#)]
10. Di Paola, A.; Bellardita, M.; Palmisano, L. Brookite, the Least Known TiO₂ Photocatalyst. *Catalysts* **2013**, *3*, 36–73. [[CrossRef](#)]
11. Cai, J.; Wang, Y.; Zhu, Y.; Wu, M.; Zhang, H.; Li, X.; Jiang, Z.; Meng, M. In Situ Formation of Disorder-Engineered TiO₂(B)-Anatase Heterophase Junction for Enhanced Photocatalytic Hydrogen Evolution. *ACS Appl. Mater. Interfaces* **2015**, *7*, 24987–24992. [[CrossRef](#)] [[PubMed](#)]
12. Li, B.-H.; Lin, Y.; Wang, J.-L.; Zhang, X.; Wang, Y.-R.; Jiang, Y.; Li, T.-S.; Liu, L.-M.; Chen, L.; Zhang, W.-L.; et al. Formation of New Phases to Improve the Visible-Light Photocatalytic Activity of TiO₂ (B) via Introducing Alien Elements. *J. Phys. Chem. C* **2017**, *121*, 52–59. [[CrossRef](#)]
13. Buckeridge, J.; Butler, K.T.; Catlow, C.R.A.; Logsdail, A.J.; Scanlon, D.O.; Shevlin, S.A.; Woodley, S.M.; Sokol, A.A.; Walsh, A. Polymorph Engineering of TiO₂: Demonstrating How Absolute Reference Potentials Are Determined by Local Coordination. *Chem. Mater.* **2015**, *27*, 3844–3851. [[CrossRef](#)]
14. Samat, M.H.; Taib, M.F.M.; Hassan, O.H.; Yahya, M.Z.A.; Ali, A.M.M. Structural, electronic and optical properties of brookite phase titanium dioxide. *Mater. Res. Express* **2017**, *4*, 44003. [[CrossRef](#)]
15. De Angelis, F.; Di Valentin, C.; Fantacci, S.; Vittadini, A.; Selloni, A. Theoretical Studies on Anatase and Less Common TiO₂ Phases: Bulk, Surfaces, and Nanomaterials. *Chem. Rev.* **2014**, *114*, 9708–9753. [[CrossRef](#)] [[PubMed](#)]
16. Linsebigler, A.L.; Lu, G.; Yates, J.T. Photocatalysis on TiO₂ Surfaces: Principles, Mechanisms, and Selected Results. *Chem. Rev.* **1995**, *95*, 735–758. [[CrossRef](#)]
17. Liu, G.; Yang, H.G.; Pan, J.; Yang, Y.Q.; Lu, G.Q.; Cheng, H.-M. Titanium Dioxide Crystals with Tailored Facets. *Chem. Rev.* **2014**, *114*, 9559–9612. [[CrossRef](#)] [[PubMed](#)]
18. Wang, X.; Li, Z.; Shi, J.; Yu, Y. One-Dimensional Titanium Dioxide Nanomaterials: Nanowires, Nanorods, and Nanobelts. *Chem. Rev.* **2014**, *114*, 9346–9384. [[CrossRef](#)] [[PubMed](#)]
19. Rietveld, H.M. A profile refinement method for nuclear and magnetic structures. *J. Appl. Crystallogr.* **1969**, *2*, 65–71. [[CrossRef](#)]

20. Gordon, T.R.; Cargnello, M.; Paik, T.; Mangolini, F.; Weber, R.T.; Fornasiero, P.; Murray, C.B. Nonaqueous Synthesis of TiO₂ Nanocrystals Using TiF₄ to Engineer Morphology, Oxygen Vacancy Concentration, and Photocatalytic Activity. *J. Am. Chem. Soc.* **2012**, *134*, 6751–6761. [[CrossRef](#)] [[PubMed](#)]
21. Romero Ocaña, I.; Beltram, A.; Delgado Jaén, J.J.; Adami, G.; Montini, T.; Fornasiero, P. Photocatalytic H₂ production by ethanol photodehydrogenation: Effect of anatase/brookite nanocomposites composition. *Inorg. Chim. Acta* **2015**, *431*, 197–205. [[CrossRef](#)]
22. Iliev, M.N.; Hadjiev, V.G.; Litvinchuk, A.P. Raman and infrared spectra of brookite (TiO₂): Experiment and theory. *Vib. Spectrosc.* **2013**, *64*, 148–152. [[CrossRef](#)]
23. Nikodemski, S.; Dameron, A.A.; Perkins, J.D.; O’Hayre, R.P.; Ginley, D.S.; Berry, J.J. The Role of Nanoscale Seed Layers on the Enhanced Performance of Niobium doped TiO₂ Thin Films on Glass. *Sci. Rep.* **2016**, *6*, 32830. [[CrossRef](#)] [[PubMed](#)]
24. Zhang, J.; Li, M.; Feng, Z.; Chen, J.; Li, C. UV Raman Spectroscopic Study on TiO₂. I. Phase Transformation at the Surface and in the Bulk. *J. Phys. Chem. B* **2006**, *110*, 927–935. [[CrossRef](#)] [[PubMed](#)]
25. Zhang, J.; Xu, Q.; Li, M.; Feng, Z.; Li, C. UV Raman Spectroscopic Study on TiO₂. II. Effect of Nanoparticle Size on the Outer/Inner Phase Transformations. *J. Phys. Chem. C* **2009**, *113*, 1698–1704. [[CrossRef](#)]
26. Buonsanti, R.; Grillo, V.; Carlino, E.; Giannini, C.; Kipp, T.; Cingolani, R.; Cozzoli, P.D. Nonhydrolytic Synthesis of High-Quality Anisotropically Shaped Brookite TiO₂ Nanocrystals. *J. Am. Chem. Soc.* **2008**, *130*, 11223–11233. [[CrossRef](#)] [[PubMed](#)]
27. Bertoni, G.; Beyers, E.; Verbeeck, J.; Mertens, M.; Cool, P.; Vansant, E.F.; Van Tendeloo, G. Quantification of crystalline and amorphous content in porous TiO₂ samples from electron energy loss spectroscopy. *Ultramicroscopy* **2006**, *106*, 630–635. [[CrossRef](#)]
28. Cargnello, M.; Montini, T.; Smolin, S.Y.; Priebe, J.B.; Delgado Jaén, J.J.; Doan-Nguyen, V.V.T.; McKay, I.S.; Schwalbe, J.A.; Pohl, M.-M.; Gordon, T.R.; et al. Engineering titania nanostructure to tune and improve its photocatalytic activity. *Proc. Natl. Acad. Sci. USA* **2016**, *113*, 3966–3971. [[CrossRef](#)] [[PubMed](#)]
29. Schneider, K.; Zajac, D.; Sikora, M.; Kapusta, C.; Michalow-Mauke, K.; Graule, T.; Rekas, M. XAS study of TiO₂-based nanomaterials. *Radiat. Phys. Chem.* **2015**, *112*, 195–198. [[CrossRef](#)]
30. Ruus, R.; Kikas, A.; Saar, A.; Ausmees, A.; Nõmmiste, E.; Aarik, J.; Aidla, A.; Uustare, T.; Martinson, I. Ti 2p and O 1s X-ray absorption of TiO₂ polymorphs. *Solid State Commun.* **1997**, *104*, 199–203. [[CrossRef](#)]
31. Angelomé, P.C.; Andriani, L.; Calvo, M.E.; Requejo, F.G.; Bilmes, S.A.; Soler-Illia, G.J.A.A. Mesoporous Anatase TiO₂ Films: Use of Ti K XANES for the Quantification of the Nanocrystalline Character and Substrate Effects in the Photocatalysis Behavior. *J. Phys. Chem. C* **2007**, *111*, 10886–10893. [[CrossRef](#)]
32. Luo, C.; Ren, X.; Dai, Z.; Zhang, Y.; Qi, X.; Pan, C. Present Perspectives of Advanced Characterization Techniques in TiO₂-Based Photocatalysts. *ACS Appl. Mater. Interfaces* **2017**, *9*, 23265–23286. [[CrossRef](#)] [[PubMed](#)]
33. Morra, E.; Giamello, E.; Chiesa, M. EPR approaches to heterogeneous catalysis. The chemistry of titanium in heterogeneous catalysts and photocatalysts. *J. Magn. Reson.* **2017**, *280*, 89–102. [[CrossRef](#)] [[PubMed](#)]
34. Keesmann, I. Zur hydrothermalen Synthese von Brookit. *Z. Anorg. Allg. Chem.* **1966**, *346*, 30–43. [[CrossRef](#)]
35. Kumar, S.G.; Rao, K.S.R.K. Polymorphic phase transition among the titania crystal structures using a solution-based approach: From precursor chemistry to nucleation process. *Nanoscale* **2014**, *6*, 11574–11632. [[CrossRef](#)] [[PubMed](#)]
36. Zhang, H.; Banfield, J.F. Structural Characteristics and Mechanical and Thermodynamic Properties of Nanocrystalline TiO₂. *Chem. Rev.* **2014**, *114*, 9613–9644. [[CrossRef](#)] [[PubMed](#)]
37. Zhang, H.; Banfield, J.F. Understanding Polymorphic Phase Transformation Behavior during Growth of Nanocrystalline Aggregates: Insights from TiO₂. *J. Phys. Chem. B* **2000**, *104*, 3481–3487. [[CrossRef](#)]
38. Ye, X.; Sha, J.; Jiao, Z.; Zhang, L. Thermoanalytical characteristic of nanocrystalline brookite-based titanium dioxide. *Nanostruct. Mater.* **1997**, *8*, 919–927. [[CrossRef](#)]
39. Su, W.; Zhang, J.; Feng, Z.; Chen, T.; Ying, P.; Li, C. Surface Phases of TiO₂ Nanoparticles Studied by UV Raman Spectroscopy and FT-IR Spectroscopy. *J. Phys. Chem. C* **2008**, *112*, 7710–7716. [[CrossRef](#)]
40. Kumar, K.-N.P.; Keizer, K.; Burggraaf, A.J.; Okubo, T.; Nagamoto, H.; Morooka, S. Densification of nanostructured titania assisted by a phase transformation. *Nature* **1992**, *358*, 48–51. [[CrossRef](#)]
41. Kominami, H.; Kohno, M.; Kera, Y. Synthesis of brookite-type titanium oxide nano-crystals in organic media. *J. Mater. Chem.* **2000**, *10*, 1151–1156. [[CrossRef](#)]

42. Ma, Y.; Xu, Q.; Chong, R.; Li, C. Photocatalytic H₂ production on TiO₂ with tuned phase structure via controlling the phase transformation. *J. Mater. Res.* **2013**, *28*, 394–399. [[CrossRef](#)]
43. Li, J.-G.; Ishigaki, T.; Sun, X. Anatase, Brookite, and Rutile Nanocrystals via Redox Reactions under Mild Hydrothermal Conditions: Phase-Selective Synthesis and Physicochemical Properties. *J. Phys. Chem. C* **2007**, *111*, 4969–4976. [[CrossRef](#)]
44. Katsumata, K.; Ohno, Y.; Tomita, K.; Taniguchi, T.; Matsushita, N.; Okada, K. Synthesis of Amphiphilic Brookite Nanoparticles with High Photocatalytic Performance for Wide Range of Application. *ACS Appl. Mater. Interfaces* **2012**, *4*, 4846–4852. [[CrossRef](#)] [[PubMed](#)]
45. Zhao, H.; Liu, L.; Andino, J.M.; Li, Y. Bicrystalline TiO₂ with controllable anatase–brookite phase content for enhanced CO₂ photoreduction to fuels. *J. Mater. Chem. A* **2013**, *1*, 8209. [[CrossRef](#)]
46. Zhao, B.; Lin, L.; He, D. Phase and morphological transitions of titania/titanate nanostructures from an acid to an alkali hydrothermal environment. *J. Mater. Chem. A* **2013**, *1*, 1659–1668. [[CrossRef](#)]
47. Manjumol, K.A.; Jayasankar, M.; Vidya, K.; Mohamed, A.P.; Nair, B.N.; Warriar, K.G.K. A novel synthesis route for brookite rich titanium dioxide photocatalyst involving organic intermediate. *J. Sol-Gel Sci. Technol.* **2015**, *73*, 161–170. [[CrossRef](#)]
48. Salari, M.; Mousavi khoie, S.M.; Marashi, P.; Rezaee, M. Synthesis of TiO₂ nanoparticles via a novel mechanochemical method. *J. Alloys Compd.* **2009**, *469*, 386–390. [[CrossRef](#)]
49. Chen, X.; Liu, L.; Huang, F. Black titanium dioxide (TiO₂) nanomaterials. *Chem. Soc. Rev.* **2015**, *44*, 1861–1885. [[CrossRef](#)] [[PubMed](#)]
50. Pan, H.; Zhang, Y.-W.; Shenoy, V.B.; Gao, H. Effects of H-, N-, and (H, N)-Doping on the Photocatalytic Activity of TiO₂. *J. Phys. Chem. C* **2011**, *115*, 12224–12231. [[CrossRef](#)]
51. Choi, M.; Lee, J.H.; Jang, Y.J.; Kim, D.; Lee, J.S.; Jang, H.M.; Yong, K. Hydrogen-doped Brookite TiO₂ Nanobullets Array as a Novel Photoanode for Efficient Solar Water Splitting. *Sci. Rep.* **2016**, *6*, 36099. [[CrossRef](#)] [[PubMed](#)]
52. Zhu, G.; Lin, T.; Lu, X.; Zhao, W.; Yang, C.; Wang, Z.; Yin, H.; Liu, Z.; Huang, F.; Lin, J. Black brookite titania with high solar absorption and excellent photocatalytic performance. *J. Mater. Chem. A* **2013**, *1*, 9650–9653. [[CrossRef](#)]
53. Xin, X.; Xu, T.; Wang, L.; Wang, C. Ti³⁺-self doped brookite TiO₂ single-crystalline nanosheets with high solar absorption and excellent photocatalytic CO₂ reduction. *Sci. Rep.* **2016**, *6*, 23684. [[CrossRef](#)] [[PubMed](#)]
54. Liu, G.; Yu, J.C.; Lu, G.Q. (Max); Cheng, H.-M. Crystal facet engineering of semiconductor photocatalysts: motivations, advances and unique properties. *Chem. Commun.* **2011**, *47*, 6763. [[CrossRef](#)] [[PubMed](#)]
55. Wen, J.; Li, X.; Liu, W.; Fang, Y.; Xie, J.; Xu, Y. Photocatalysis fundamentals and surface modification of TiO₂ nanomaterials. *Cuihua Xuebao Chin. J. Catal.* **2015**, *36*, 2049–2070. [[CrossRef](#)]
56. Kumar, S.G.; Rao, K.S.R.K. Comparison of modification strategies towards enhanced charge carrier separation and photocatalytic degradation activity of metal oxide semiconductors (TiO₂, WO₃ and ZnO). *Appl. Surf. Sci.* **2017**, *391*, 124–148. [[CrossRef](#)]
57. Vequizo, J.J.M.; Matsunaga, H.; Ishiku, T.; Kamimura, S.; Ohno, T.; Yamakata, A. Trapping-Induced Enhancement of Photocatalytic Activity on Brookite TiO₂ Powders: Comparison with Anatase and Rutile TiO₂ Powders. *ACS Catal.* **2017**. [[CrossRef](#)]
58. Moss, B.; Lim, K.K.; Beltram, A.; Moniz, S.; Tang, J.; Fornasiero, P.; Barnes, P.; Durrant, J.; Kafizas, A. Comparing photoelectrochemical water oxidation, recombination kinetics and charge trapping in the three polymorphs of TiO₂. *Sci. Rep.* **2017**, *7*, 2938. [[CrossRef](#)] [[PubMed](#)]
59. Na-Phattalung, S.; Smith, M.F.; Kim, K.; Du, M.-H.; Wei, S.-H.; Zhang, S.B.; Limpijumnong, S. First-principles study of native defects in anatase TiO₂. *Phys. Rev. B* **2006**, *73*, 125205. [[CrossRef](#)]
60. Mattioli, G.; Filippone, F.; Alippi, P.; Amore Bonapasta, A. Ab initio study of the electronic states induced by oxygen vacancies in rutile and anatase TiO₂. *Phys. Rev. B* **2008**, *78*, 241201. [[CrossRef](#)]
61. Yamakata, A.; Vequizo, J.J.M.; Matsunaga, H. Distinctive Behavior of Photogenerated Electrons and Holes in Anatase and Rutile TiO₂ Powders. *J. Phys. Chem. C* **2015**, *119*, 24538–24545. [[CrossRef](#)]
62. Li, L.; Salvador, P.A.; Rohrer, G.S. Photocatalysts with internal electric fields. *Nanoscale* **2014**, *6*, 24–42. [[CrossRef](#)] [[PubMed](#)]
63. Henderson, M.A. A surface science perspective on TiO₂ photocatalysis. *Surf. Sci. Rep.* **2011**, *66*, 185–297. [[CrossRef](#)]

64. Lin, H.; Li, L.; Zhao, M.; Huang, X.; Chen, X.; Li, G.; Yu, R. Synthesis of High-Quality Brookite TiO₂ Single-Crystalline Nanosheets with Specific Facets Exposed: Tuning Catalysts from Inert to Highly Reactive. *J. Am. Chem. Soc.* **2012**, *134*, 8328–8331. [[CrossRef](#)] [[PubMed](#)]
65. Pepin, P.A.; Diroll, B.T.; Choi, H.J.; Murray, C.B.; Vohs, J.M. Thermal and Photochemical Reactions of Methanol, Acetaldehyde, and Acetic Acid on Brookite TiO₂ Nanorods. *J. Phys. Chem. C* **2017**, *121*, 11488–11498. [[CrossRef](#)]
66. Naldoni, A.; Montini, T.; Malara, F.; Mróz, M.M.; Beltram, A.; Virgili, T.; Boldrini, C.L.; Marelli, M.; Romero-Ocaña, I.; Delgado, J.J.; et al. Hot Electron Collection on Brookite Nanorods Lateral Facets for Plasmon-Enhanced Water Oxidation. *ACS Catal.* **2017**, *7*, 1270–1278. [[CrossRef](#)]
67. Gong, X.-Q.; Selloni, A. First-principles study of the structures and energetics of stoichiometric brookite TiO₂. *Phys. Rev. B* **2007**, *76*, 235307. [[CrossRef](#)]
68. Ohno, T.; Higo, T.; Saito, H.; Yuajn, S.; Jin, Z.; Yang, Y.; Tsubota, T. Dependence of photocatalytic activity on aspect ratio of a brookite TiO₂ nanorod and drastic improvement in visible light responsibility of a brookite TiO₂ nanorod by site-selective modification of Fe³⁺ on exposed faces. *J. Mol. Catal. A Chem.* **2015**, *396*, 261–267. [[CrossRef](#)]
69. Ohno, T.; Sarukawa, K.; Matsumura, M. Crystal faces of rutile and anatase TiO₂ particles and their roles in photocatalytic reactions. *New J. Chem.* **2002**, *26*, 1167–1170. [[CrossRef](#)]
70. Ohno, T.; Higo, T.; Murakami, N.; Saito, H.; Zhang, Q.; Yang, Y.; Tsubota, T. Photocatalytic reduction of CO₂ over exposed-crystal-face-controlled TiO₂ nanorod having a brookite phase with co-catalyst loading. *Appl. Catal. B Environ.* **2014**, *152*, 309–316. [[CrossRef](#)]
71. Zhao, M.; Xu, H.; Chen, H.; Ouyang, S.; Umezawa, N.; Wang, D.; Ye, J. Photocatalytic reactivity of {121} and {211} facets of brookite TiO₂ crystals. *J. Mater. Chem. A* **2015**, *3*, 2331–2337. [[CrossRef](#)]
72. Xu, Y.; Lin, H.; Li, L.; Huang, X.; Li, G. Precursor-directed synthesis of well-faceted brookite TiO₂ single crystals for efficient photocatalytic performances. *J. Mater. Chem. A* **2015**, *3*, 22361–22368. [[CrossRef](#)]
73. Kapilashrami, M.; Zhang, Y.; Liu, Y.-S.; Hagfeldt, A.; Guo, J. Probing the Optical Property and Electronic Structure of TiO₂ Nanomaterials for Renewable Energy Applications. *Chem. Rev.* **2014**, *114*, 9662–9707. [[CrossRef](#)] [[PubMed](#)]
74. Li, G.; Gray, K.A. The solid–solid interface: Explaining the high and unique photocatalytic reactivity of TiO₂-based nanocomposite materials. *Chem. Phys.* **2007**, *339*, 173–187. [[CrossRef](#)]
75. Kawahara, T.; Konishi, Y.; Tada, H.; Tohge, N.; Nishii, J.; Ito, S. A Patterned TiO₂(Anatase)/TiO₂(Rutile) Bilayer-Type Photocatalyst: Effect of the Anatase/Rutile Junction on the Photocatalytic Activity. *Angew. Chem.* **2002**, *15*, 2935–2937. [[CrossRef](#)]
76. Hurum, D.C.; Agrios, A.G.; Gray, K.A.; Rajh, T.; Thurnauer, M.C. Explaining the Enhanced Photocatalytic Activity of Degussa P25 Mixed-Phase TiO₂ Using EPR. *J. Phys. Chem. B* **2003**, *107*, 4545–4549. [[CrossRef](#)]
77. Shen, X.; Zhang, J.; Tian, B.; Anpo, M. Tartaric acid-assisted preparation and photocatalytic performance of titania nanoparticles with controllable phases of anatase and brookite. *J. Mater. Sci.* **2012**, *47*, 5743–5751. [[CrossRef](#)]
78. Ardizzone, S.; Bianchi, C.L.; Cappelletti, G.; Gialanella, S.; Pirola, C.; Ragaini, V. Tailored Anatase/Brookite Nanocrystalline TiO₂. The Optimal Particle Features for Liquid- and Gas-Phase Photocatalytic Reactions. *J. Phys. Chem. C* **2007**, *111*, 13222–13231. [[CrossRef](#)]
79. Xu, H.; Zhang, L. Controllable One-Pot Synthesis and Enhanced Photocatalytic Activity of Mixed-Phase TiO₂ Nanocrystals with Tunable Brookite/Rutile Ratios. *J. Phys. Chem. C* **2009**, *113*, 1785–1790. [[CrossRef](#)]
80. Boppella, R.; Basak, P.; Manorama, S.V. Viable Method for the Synthesis of Biphasic TiO₂ Nanocrystals with Tunable Phase Composition and Enabled Visible-Light Photocatalytic Performance. *ACS Appl. Mater. Interfaces* **2012**, *4*, 1239–1246. [[CrossRef](#)] [[PubMed](#)]
81. Li, W.-K.; Hu, P.; Lu, G.; Gong, X.-Q. Density functional theory study of mixed-phase TiO₂: Heterostructures and electronic properties. *J. Mol. Model.* **2014**, *20*, 2215. [[CrossRef](#)] [[PubMed](#)]
82. Kandiel, T.A.; Feldhoff, A.; Robben, L.; Dillert, R.; Bahnemann, D.W. Tailored Titanium Dioxide Nanomaterials: Anatase Nanoparticles and Brookite Nanorods as Highly Active Photocatalysts. *Chem. Mater.* **2010**, *22*, 2050–2060. [[CrossRef](#)]
83. Li, Z.; Cong, S.; Xu, Y. Brookite vs Anatase TiO₂ in the Photocatalytic Activity for Organic Degradation in Water. *ACS Catal.* **2014**, *4*, 3273–3280. [[CrossRef](#)]

84. Li, W.-K.; Gong, X.-Q.; Lu, G.; Selloni, A. Different Reactivities of TiO₂ Polymorphs: Comparative DFT Calculations of Water and Formic Acid Adsorption at Anatase and Brookite TiO₂ Surfaces. *J. Phys. Chem. C* **2008**, *112*, 6594–6596. [[CrossRef](#)]
85. Rodriguez, M.M.; Peng, X.; Liu, L.; Li, Y.; Andino, J.M. A Density Functional Theory and Experimental Study of CO₂ Interaction with Brookite TiO₂. *J. Phys. Chem. C* **2012**, *116*, 19755–19764. [[CrossRef](#)]
86. Liu, L.; Zhao, H.; Andino, J.M.; Li, Y. Photocatalytic CO₂ Reduction with H₂O on TiO₂ Nanocrystals: Comparison of Anatase, Rutile, and Brookite Polymorphs and Exploration of Surface Chemistry. *ACS Catal.* **2012**, *2*, 1817–1828. [[CrossRef](#)]
87. Livraghi, S.; Rolando, M.; Maurelli, S.; Chiesa, M.; Paganini, M.C.; Giamello, E. Nature of Reduced States in Titanium Dioxide as Monitored by Electron Paramagnetic Resonance. II: Rutile and Brookite Cases. *J. Phys. Chem. C* **2014**, *118*, 22141–22148. [[CrossRef](#)]
88. Livraghi, S.; Chiesa, M.; Paganini, M.C.; Giamello, E. On the Nature of Reduced States in Titanium Dioxide As Monitored by Electron Paramagnetic Resonance. I: The Anatase Case. *J. Phys. Chem. C* **2011**, *115*, 25413–25421. [[CrossRef](#)]
89. Palmisano, G.; Garcia-Lopez, E.; Marci, G.; Loddo, V.; Yurdakal, S.; Augugliaro, V.; Palmisano, L. Advances in selective conversions by heterogeneous photocatalysis. *Chem. Commun.* **2010**, *46*, 7074–7089. [[CrossRef](#)] [[PubMed](#)]
90. Zhang, X.; Xiong, X.; Xu, Y. Brookite TiO₂ photocatalyzed degradation of phenol in presence of phosphate, fluoride, sulfate and borate anions. *RSC Adv.* **2016**, *6*, 61830–61836. [[CrossRef](#)]
91. Kou, J.; Lu, C.; Wang, J.; Chen, Y.; Xu, Z.; Varma, R.S. Selectivity Enhancement in Heterogeneous Photocatalytic Transformations. *Chem. Rev.* **2017**, *117*, 1445–1514. [[CrossRef](#)] [[PubMed](#)]
92. Altomare, M.; Dozzi, M.V.; Chiarello, G.L.; Di Paola, A.; Palmisano, L.; Selli, E. High activity of brookite TiO₂ nanoparticles in the photocatalytic abatement of ammonia in water. *Catal. Today* **2015**, *252*, 184–189. [[CrossRef](#)]
93. Addamo, M.; Augugliaro, V.; Bellardita, M.; Di Paola, A.; Loddo, V.; Palmisano, G.; Palmisano, L.; Yurdakal, S. Environmentally Friendly Photocatalytic Oxidation of Aromatic Alcohol to Aldehyde in Aqueous Suspension of Brookite TiO₂. *Catal. Lett.* **2008**, *126*, 58–62. [[CrossRef](#)]
94. Li, K.; Peng, T.; Ying, Z.; Song, S.; Zhang, J. Ag-loading on brookite TiO₂ quasi nanocubes with exposed {210} and {001} facets: Activity and selectivity of CO₂ photoreduction to CO/CH₄. *Appl. Catal. B Environ.* **2016**, *180*, 130–138. [[CrossRef](#)]
95. Karimipour, M.; Sanjari, M.; Molaei, M. The synthesis of highly oriented brookite nanosheets using graphene oxide as a sacrificing template. *J. Mater. Sci. Mater. Electron.* **2017**, *28*, 9410–9415. [[CrossRef](#)]
96. Yuan, H.; Han, K.; Dubbink, D.; Mul, G.; ten Elshof, J.E. Modulating the External Facets of Functional Nanocrystals Enabled by Two-Dimensional Oxide Crystal Templates. *ACS Catal.* **2017**, 6858–6863. [[CrossRef](#)]
97. Li, K.; Peng, B.; Jin, J.; Zan, L.; Peng, T. Carbon nitride nanodots decorated brookite TiO₂ quasi nanocubes for enhanced activity and selectivity of visible-light-driven CO₂ reduction. *Appl. Catal. B Environ.* **2017**, *203*, 910–916. [[CrossRef](#)]
98. Shang, Q.; Huang, X.; Tan, X.; Yu, T. High Activity Ti³⁺-Modified Brookite TiO₂/Graphene Nanocomposites with Specific Facets Exposed for Water Splitting. *Ind. Eng. Chem. Res.* **2017**, *56*, 9098–9106. [[CrossRef](#)]
99. Anpo, M.; Yamashita, H.; Ichihashi, Y.; Fujii, Y.; Honda, M. Photocatalytic Reduction of CO₂ with H₂O on Titanium Oxides Anchored within Micropores of Zeolites: Effects of the Structure of the Active Sites and the Addition of Pt. *J. Phys. Chem. B* **1997**, *101*, 2632–2636. [[CrossRef](#)]
100. Chen, T.; Dong, B.; Chen, K.; Zhao, F.; Cheng, X.; Ma, C.; Lee, S.; Zhang, P.; Kang, S.H.; Ha, J.W.; et al. Optical Super-Resolution Imaging of Surface Reactions. *Chem. Rev.* **2017**, *117*, 7510–7537. [[CrossRef](#)] [[PubMed](#)]
101. Tachikawa, T.; Yonezawa, T.; Majima, T. Super-Resolution Mapping of Reactive Sites on Titania-Based Nanoparticles with Water-Soluble Fluorogenic Probes. *ACS Nano* **2013**, *7*, 263–275. [[CrossRef](#)] [[PubMed](#)]
102. Zhong, H.; Zhang, J.; Tang, X.; Zhang, W.; Jiang, R.; Li, R.; Chen, D.; Wang, P.; Yuan, Z. Mass spectrometric monitoring of interfacial photoelectron transfer and imaging of active crystalline facets of semiconductors. *Nat. Commun.* **2017**, *8*, 14524. [[CrossRef](#)] [[PubMed](#)]
103. Li, K.; Peng, B.; Peng, T. Recent Advances in Heterogeneous Photocatalytic CO₂ Conversion to Solar Fuels. *ACS Catal.* **2016**, *6*, 7485–7527. [[CrossRef](#)]
104. Magne, C.; Cassaignon, S.; Lancel, G.; Pauporté, T. Brookite TiO₂ Nanoparticle Films for Dye-Sensitized Solar Cells. *ChemPhysChem* **2011**, *12*, 2461–2467. [[CrossRef](#)] [[PubMed](#)]

105. Xu, J.; Wu, S.; Jin, J.; Peng, T. Preparation of brookite TiO₂ nanoparticles with small sizes and the improved photovoltaic performance of brookite-based dye-sensitized solar cells. *Nanoscale* **2016**, *8*, 18771–18781. [[CrossRef](#)] [[PubMed](#)]
106. Liu, K.; Cao, M.; Fujishima, A.; Jiang, L. Bio-Inspired Titanium Dioxide Materials with Special Wettability and Their Applications. *Chem. Rev.* **2014**, *114*, 10044–10094. [[CrossRef](#)] [[PubMed](#)]
107. Shibata, T.; Irie, H.; Ohmori, M.; Nakajima, A.; Watanabe, T.; Hashimoto, K. Comparison of photochemical properties of brookite and anatase TiO₂ films. *Phys. Chem. Chem. Phys.* **2004**, *6*, 1359–1362. [[CrossRef](#)]



© 2017 by the authors. Licensee MDPI, Basel, Switzerland. This article is an open access article distributed under the terms and conditions of the Creative Commons Attribution (CC BY) license (<http://creativecommons.org/licenses/by/4.0/>).